Journal of Molecular Structure 1271 (2023) 134076

Contents lists available at ScienceDirect

Journal of Molecular Structure

journal homepage: www.elsevier.com/locate/molstr

Novel reduced graphene oxide/zinc phthalocyanine and reduced graphene oxide/cobalt phthalocyanine hybrids as high sensitivity room temperature volatile organic compound gas sensors

Ebru Yabaş[a,*], Emre Biçer[b], Ahmet Altındal[c]

[a] Advanced Technology Application and Research Center, Sivas Cumhuriyet University, 58140, Sivas, Turkey
[b] Faculty of Engineering and Natural Sciences, Sivas University of Science and Technology, 58140, Sivas, Turkey
[c] Faculty of Arts and Sciences, Department of Physics, Yıldız Technical University, 34220, İstanbul, Turkey

ARTICLE INFO

Article history:
Received 16 May 2022
Revised 23 August 2022
Accepted 1 September 2022
Available online 2 September 2022

Keywords:
Metallophthalocyanine
Graphene oxide
Hybrid
Gas sensor
Ammonia

ABSTRACT

In this work, novel 4-pyridynyl-oxadiazole tetrasubstituted zinc and cobalt phthalocyanine compounds were synthesized and characterized by UV-vis, Fluorescence spectroscopy, and SEM. Then these compounds were mixed with reduced graphene oxide. As a result of the interaction of these newly synthesized phthalocyanines with reduced graphene oxide (rGO), rGO/ZnPc and rGO/CoPc hybrids were obtained. The measurement results confirm that the prepared non-covalent rGO/ZnPc and rGO/CoPc hybrid structures are formed by strong $\pi-\pi$ interaction. A comparative study of the sensor response of rGO and non-covalently functionalized with zinc and cobalt phthalocyanines (rGO/ZnPc, and rGO/CoPc) hybrids to five different volatile organic compound vapors, ammonia, acetone, ethanol, methanol and butanol is carried out. The response of the sensors increases with respect to ammonia concentrations ranging from 30 to 210 ppm. The response time for 120 ppm ammonia vapor were approximately 250s, 230s and 190s for rGO, rGO/ZnPc, and rGO/CoPc based sensors, respectively. Also, we have conducted selectivity experiments with the aforementioned vapors, thus, studies have indicated that functionalization of rGO with ZnPc results in a 43-fold improvement in sensor response towards ammonia vapors.

1. Introduction

Phthalocyanines (Pc) are macrocyclic compounds incorporated with porphyrin ring connected with isoindole groups, with two pyrrolic hydrogen atoms in a non-substituted form (H_2Pc) with delocalized 18π-electrons and a two-dimensional geometry. Substitution of these pyrrolic hydrogen atoms with metal atoms gives rise to coordination compound metallophthalocyanines (MPcs). Phthalocyanines receive a considerable attention due to their exciting properties allowing using in a variety of applications in electronics, sensors, semiconductors, catalysis, and photovoltaics. Phthalocyanines demonstrate many different properties according to different metals attached on the center of the molecule and also according to substituents attached to organic core structure [1]. MPcs are also intensively studied by researchers due to its wide range of applications. MPcs with highly electronic delocalization let them use in semiconductor materials. Also, with planar conjugated skeleton, MPcs exhibit highly thermal and chemical stability. On the other hand, it is known that aromatic oxadiazole-based compounds, which facilitate electron injection and transport, have high electron affinities. Oxadiazoles and its derivatives, which belong to the class of heterocyclic compounds, have a strong tendency to sensing in the sensor applications [2]. It is expected that the new molecules to be obtained by the combination of these two groups of compounds, which are very active in sensor applications, will also show effective properties. MPcs also provide an incorporation with graphene by π-π interactions (non-covalent) or covalent modification [3].

Graphene is also, with its two-dimensional monolayer and sp^2-hybridized structure, the most promising material to be used in many applications efficiently. However, obtaining a pure graphene is not very easy. Graphene is obtained from graphite by Hummers method [4]. But after this method the obtained is not graphene, its oxidized state: graphene oxide (GO). Unlike graphene, GO does not have excellent properties like electrical, optical and thermal conductivity. However, incorporation of molecules on graphene oxide is quite easy since there are functional groups such as hydroxy, carboxy, epoxy to attach molecules. After attaching molecules, unreacted functional groups can be reduced in different ways by thermal, chemical or physically. This excellent property makes

* Corresponding author.
E-mail address: eyabas@cumhuriyet.edu.tr (E. Yabaş).

https://doi.org/10.1016/j.molstruc.2022.134076
0022-2860/

graphene oxide very popular since (i) easy tunability of chemical properties (ii) anchoring different substrates to tune the chemical property [5]. On the other hand, studies on the preparation of thin-film gas sensors using novel nanomaterials with advanced functionality for the detection of VOC gases have attracted great interest in the literature [5–8].

Functional modification of graphene with metallophthalocyanine is a very promising way to enhance the properties of the π-π stacked hybrid structure. Different metallophthalocyanine with different metals may demonstrate interesting properties in gas sensing applications [9]. Guo et al. reported a highly sensitive ammonia sensor by using cobalt phthalocyanine with different phenoxyl substituents stacked with rGO able to sense in ppb levels. They found out that carboxyl groups on the phenoxyl substituents give rise to NH_3 adsorption [8]. Zhou et al., on the other hand, proposed copper phthalocyanines anchored to the surface of rGO demonstrating ammonia gas sensing with different concentrations (400 ppb to 3200 ppm) [5]. Wang also studied on the sensing performance of NH_3 by using CoPc with different amino substituents tailored on the surface of rGO [10]. This hybrid structure was also tested with a series of volatile organic compounds (VOC) and NOx. The performance of the hybrid structure was found to be excellent due to the presence of amino groups with strong electron-donor effect. Also, Li et al. demonstrated the effect of different metal centers of Pc with rGO. The best performance on the response time was found to be with nickel substituted Pc and best recovery time with rGO/CuPc among copper, nickel and lead. It is declared that these rGO/MPc hybrid structures had a weak response to CO_2, CO, CH_4 and H_2 [11]. Yu et al. performed gas sensing experiments with 1,8,15,22-tetra-(4-tert-butylphenoxyl) metallophthalocyanine (TBPOMPc, M:Cu, Ni, Pb) together with rGO towards ammonia, CO, NO_2 and H_2 and exposed a strong selectivity to ammonia [12]. Another rGO/MPc sensor structures was studied with Kumar et al. His research group, on the other hand, conducted Cl_2 detection in ppb levels. rGO/CuPc nanoflower hybrid structures stacked by non-covalent π-π interactions demonstrated a great selectivity towards Cl_2 compared to other NO_2, NO and NH_3 [13]. The sensing mechanism was displayed with electrochemical impedance spectroscopy (EIS). All the studies mentioned performed a better performance with hybrid structures of rGO/MPc compared with rGO. It is obvious that MPcs display active sites for adsorption of gas molecules and also rGO presents high surface area.

As a 2D carbon-based material, reduced graphene oxide has become a focus of attention especially in gas sensing applications due to its high surface-to-volume ratio, tunable electrical and optical properties. Although reduced graphene oxide-based sensors show sensitivity to different gases such as H_2S, NH_3, Cl_2, NO, their selectivity, sensitivity and recovery to original baseline still remain a challenge [13–16]. More recently, it was shown that functional modification of rGO surface is an effective way to overcome the issues of poor selectivity, slow response and recovery times in rGO based sensors [[17],[18]]. Metallophthalocyanines (MPcs) have been identified as promising sensing element in chemiresistive based sensors for the detection of various gases [[19],[20]], due to their π- conjugated skeleton, tunability of electrical and gas sensing properties by manipulation of the central metal ion and by substitution of functional groups. In addition, another advantage of MPcs is their high tendency with carbon-based materials such as reduced graphene oxide, since the presence of active substituent groups in the structure of MPcs enhances through covalent or non-covalent interactions with carbon-based materials.

VOC sensors are of interest in many fields, from medicine to the preparation of advanced technological materials. For example, human breath contains, in addition to oxygen, nitrogen, carbon dioxide and water vapor, different types and concentrations of volatile organic compounds in the presence of certain diseases [21–24]. In this way, it is possible to provide non-invasive, painless and capable of rapid response, low-cost and easily reproducible medical diagnosis with breath analysis [25–28]. The development of a sensor that can analyze the chemical composition of human breath will be an alternative and innovative initiative, especially for the early detection of ailments in lung, kidney, stomach or in other body parts [[21],[22],[29]]. In recent years, the development of such devices that can be used practically has also aroused great interest. For instance, kidney failure is a clinically silent disease that does not manifest itself until the advanced stage. Early diagnosis of this disease, which causes irreversible loss of kidney function, can only be characterized by an increase in ammonia concentration of several hundred ppb in breath analysis [21].

Based on the above consideration, we synthesized novel 4-pyridynyl-oxadiazole tetrasubstituted zinc and cobalt phthalocyanine compounds and prepared hybrids as a result of the interaction of these compounds with rGO. Then, we conducted gas sensing studies with MPcs by non-covalently furnished on rGO. According to our knowledge, rGO/ZnPc and rGO/CoPc hybrid materials are novel on gas sensing applications especially on NH_3 and volatile organic compound such as acetone, ethanol, methanol, and butanol.

2. Experimental

2.1. General

All solvents used in synthesis reactions carried out under nitrogen atmosphere were dried by molecular sieves or suitable methods [30]. The oxadiazole derivative substituted phthalonitrile derivative as starting material was synthesized according to the literature [31]. rGO/ZnPc and rGO/CoPc hybrid solutions were prepared in a sonicator. Sonics VCX-750 Vibra Cell was used for the sonication process. The absorption and fluorescence spectra were recorded by a Shimadzu UV-1800 spectrophotometer and Agilent Cary Eclipse G9800A Fluorescence Spectrometer, respectively. FT-IR analysis was conducted by Bruker Tensor II FT-IR spectrophotometer. FT-IR spectra were measured by preparing a KBr pellet. SEM images were examined with a TESCAN® MIRA3 XMU (Brno, Czechia) brand scanning electron microscope. Electrothermal 9100 digital melting point apparatus was used to determine the melting point.

2.2. Synthesis of ZnPc

Oxadiazole substituted phthalonitrile (100.0 mg, 0.34 mmol) and $Zn(OAc)_2.2H_2O$ (18.7 mg, 0.085 mmol) were mixed in DMF (3 mL) under nitrogen gas at room temperature. This mixture was heated at 185 °C for 24 h in the presence of 1,8-diazabicyclo[5.4.0]undec-7-ene (DBU). After the reaction was completed, the mixture was cooled; the organic phase was precipitated with MeOH and filtered. The crude product was washed with water, MeOH, and then dried. Then the green solid was washed with acetone using the soxhlet apparatus and dried in vacuum. The purified green compound was soluble in THF, DMF and DMSO. Yield 38% (40.0 mg). Mp: >300 °C. ^{1}H-NMR (400 MHz, DMSO-d_6) δ = 8.9-8.1 (br, 12H, Pc Ar-H); 8.0-7.6 (br, 16H, pyridyl Ar-H). UV-vis (DMSO) λ_{max}/nm 687, 632, 357. IR (KBr pellet) υ (cm^{-1}) 3062, 1642, 1601, 1486, 1441, 1098, 1075, 763, 700. Anal. Calc. for $C_{60}H_{28}N_{20}O_4S_4Zn$: C 54.28; H 2.13; N 21.10; S 9.66%, found: C 54.43; H 2.26; N 21.41; S 9.52%. MALDI-TOF MS m/z: 1288 $[M+H]^+$.

2.3. Synthesis of CoPc

Oxadiazole substituted phthalonitrile (100.0 mg, 0.34 mmol) and $Co(OAc)_2.4H_2O$ (21.2 mg, 0.085 mmol) were mixed in DMF

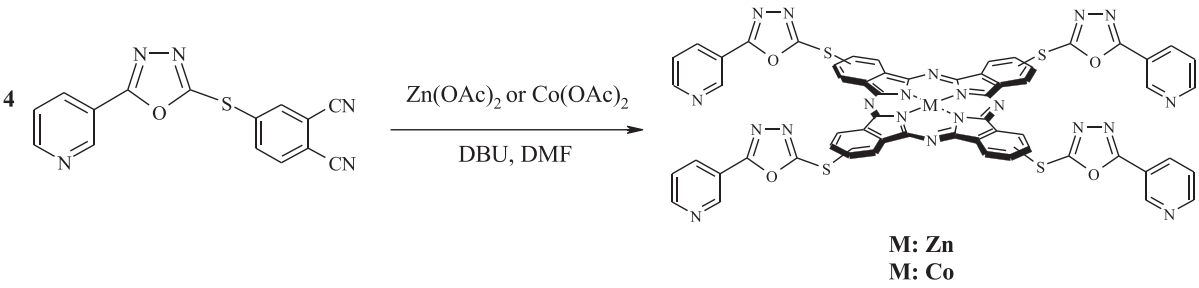

Scheme 1. The synthesis of ZnPc and CoPc.

(3 mL) under nitrogen gas at room temperature. This mixture was heated at 185 °C for 20 h in the presence of DBU. After the reaction was completed, the mixture was cooled and the product was purified using the purification method applied for compound **1**. The purified green compound was soluble in THF, DMF and DMSO. Yield 36% (38.0 mg). Mp: >300 °C. UV-vis (DMSO) λ_{max}/nm 679, 618, 340. IR (KBr pellet) υ (cm^{-1}) 3060, 1646, 1601, 1487, 1446, 1098, 1074, 764, 745. Anal. Calc. for $C_{60}H_{28}N_{20}O_4S_4Co$: C 56.29; H 2.20; N 21.88; S 10.02%, found: C 56.43; H 2.29; N 21.95; S 10.17%. MALDI-TOF MS m/z: 1281 $[M+H]^+$.

2.4. Synthesis of rGO/ZnPc and rGO/CoPc hybrids

rGO solutions (0.00005 μg/mL; 0.0005 μg/mL; 0.005 μg/mL; 0.05 μg/mL; 0.5 μg/mL; 0.7 μg/mL; 1 μg/mL) were prepared by sonication in DMSO. The solution of 5 μg/mL of ZnPc or CoPc in DMSO (5 mL) was added to different concentrations of rGO solutions (5 mL), respectively. The prepared solutions were sonicated for 25 min.

2.5. Surface analysis

Solvent of rGO/MPc hybrids prepared by sonication in solution phase at 1 μg/mL / 5 μg/mL ratios was removed in the evaporator. The images of the obtained rGO/MPc hybrids were taken in powder form by scanning electron microscopy.

2.6. Sensing experiments

In gas sensing experiments, gold interdigital electrode structure consisting of 25 finger pairs with a finger spacing of 50 μ and finger width of 50 μ was used as transducer. As described in our previous studies [32], an entire description of the gas sensing set-up is shown in Fig. 1. To prepare thin film of sensing layers, as prepared rGO/MPc hybrids were dispersed by ultrasonication in tetrahydrofuran (THF) for 3 h, and then 100 μl of dispersion was spin coated on the inderdigated gold electrodes. After the spin coating at 2500 rpm, thin film of the rGO/MPc hybrids were heat treated at 90 °C for 3 h in a vacuum oven to ensure that no solvent was left in the films. A systematic study has been performed to optimize the sensing film thickness. For this purpose, films were prepared at speeds varying between 1000 and 4000 rpm, and the maximum sensor response was obtained with films prepared at 2500 rpm. Therefore, 2500 rpm was used as the spin speed for all films. The dependence of the final film thickness on the inverse square root of the spin speed is the most common reported experimental relationship between these two quantities [33]. Taking into account this relationship between film thickness and spin speed, the thickness of the sensing layer formed at 2500 rpm were estimated as 210 nm.

In order to test the sensing performance of the films towards five different volatile organic compounds (NH_3, acetone, ethanol, methanol, and butanol), the sensors were placed in a stainless-steel chamber with a volume of 5×10^{-4} L. The ammonia vapours were generated from the cooled bubblers (saturation vapor pressures were calculated using Antoine equation [34] with dry nitrogen as carrier gas and passed through stainless steel tubing in a water bath to adjust the gas temperature. The gas streams were diluted with dry nitrogen to adjust the desired ammonia concentration with computer driven MFCs. A typical sensing test cycle composed of three sequential steps. First, the sensors were exposed to carrier gas (in our case, 99.9% pure dry nitrogen) at a flow rate of 100 sccm for 4 h to obtain a baseline. Later, the sensors were exposed to a well-defined concentration of target molecules for 5 min., which was obtained by bubbling of carrier gas through ultra-pure liquid phase of the target molecules using computer driven mass flow controllers (Alicat Scientific, Inc.) (see Fig. 1). Finally, the sensor was recovered in the carrier gas ambient for another 5 min. During the sensing experiments, the total gas flow rate was set as 100 sccm in all measurements in order to eliminate the flow rate and therefore the pressure effect.

3. Results and discussion

3.1. Synthesis and characterization

The synthesis of novel tetra-substituted zinc and cobalt phthalocyanines were undergone by 4-pyridynyl-oxadiazole substituted phthalonitrile with zinc acetate and cobalt(II) acetate in stochiometric amounts in DMF medium by using DBU as a base at 185 °C (Scheme 1). The yields were found to be 38% and 36% for ZnPc and CoPc, respectively, based on the amount of phthalonitrile used. The characterization of the ZnPc was realized by NMR with the characteristic aromatic peaks of phenyl and pyridinyl groups 8.9-8.1 and at 8.0-7.6 ppm, respectively. However, we could not have any meaningful NMR data from CoPc, since the para-magnetic nature of the compound precluded the peak separation [35].

In the FT-IR spectrum of the phthalonitrile derivative, the band of the -C≡N observed at 2241 cm^{-1} [31] and then, disappeared in ZnPc and CoPc. This confirms that the tetramerization reaction has taken place and the starting material has totally been consumed. In the spectrum of both compounds were observed 1646-1601 cm^{-1} for the stretching vibration of C=C, 1487–1441 cm^{-1} for the stretching vibrations of C=N, 1098-1074 cm^{-1} for the stretching vibrations of N-N and also 763–700 cm^{-1} for the stretching vibrations of C-S-C [[31],[36–39]].

In UV-Vis spectra of both macromolecules ZnPc and CoPc the characteristic Q-bands which showing the metal complexation of phthalocyanine was observed at 687 and 679 nm for Zn and Co phthalocyanine, respectively. Thus, we confirmed that we are successful on metallation of phthalocyanines [40]. Also, B-bands were appeared at 357 and 340 nm for ZnPc and CoPc, respectively. The elemental analysis results of the compounds are in good agreement with the calculated results of the molecules.

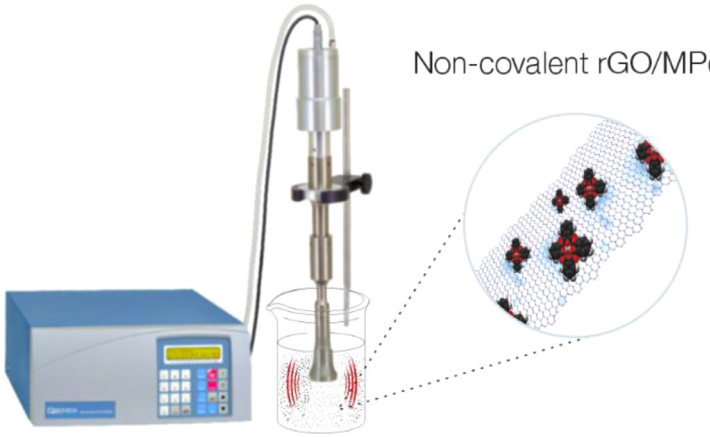

Scheme 2. The preparation of rGO/ZnPc and rGO/CoPc hybrids.

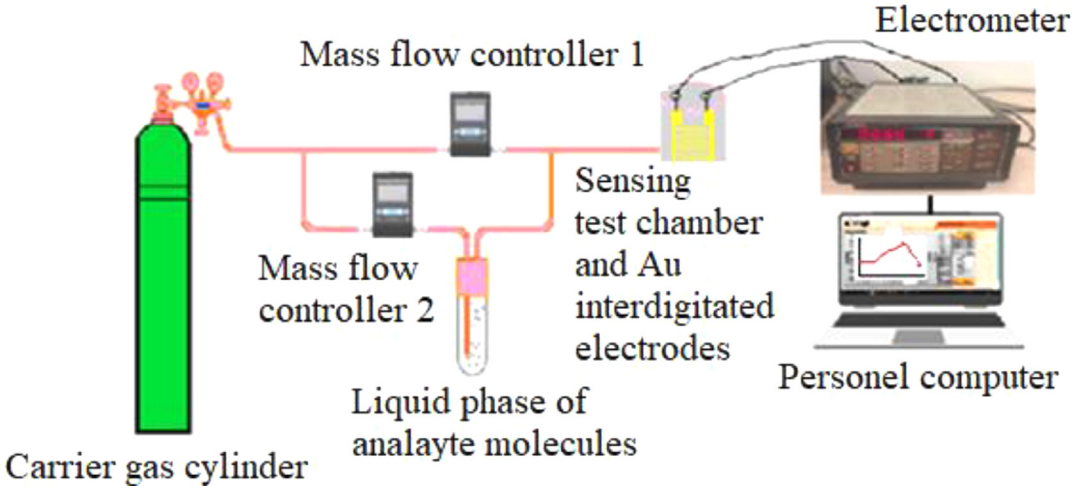

Fig. 1. Gas sensing experimental set-up.

After successful synthesis of ZnPc and CoPc, a sonication process was applied to anchor these macromolecules on the surface of rGO through $\pi-\pi$ interaction (Scheme 2). Various concentrations were prepared in DMSO to provide the adequate interaction between the macromolecules and rGO and also to prevent the aggregation of ZnPc and CoPc on the surface of rGO. The absorption spectra of rGO/ZnPc and rGO/CoPc hybrids were depicted in Fig. 2. According to rGO/ZnPc spectra, increasing amount of rGO shifts the peak intensity from 687 nm (no rGO added) to 721 nm (rGO concentration 1 μg/mL). This shift accounts to $\pi-\pi$ interaction illustrating the flattening of the curves by the increasing amount of rGO [41]. After the formation of rGO/ZnPc and rGO/CoPc hybrid structures, a redshift of 34 nm and 29 nm were respectively observed in UV-Vis spectra. It was observed that the redshift observed with the formation of the rGO/ZnPc hybrid was higher than that of the rGO/CoPc hybrid.

Fluorescence spectra of rGO/ZnPc and rGO/CoPc hybrids were illustrated in Fig. 3A and 3B, respectively. Solutions in different concentrations of rGO (0.005 μg/mL; 0.05 μg/mL; 0.5 μg/mL; 1 μg/mL) were added separately to the solution of MPc (5 μg/mL), and then sonication process was applied. The changes in emission spectra of rGO/MPc hybrid derivatives prepared at varying concentration ratios of rGO were investigated. The emission intensity gradually decreased by increasing rGO concentration in both hybrid structures and the emission peak shifted to the lower wavelength. This effect indicates the effective energy transfer from phthalocyanine to rGO. No change was observed in the emission peak with rGO concentration above 1 μg/mL. After observation of the fluorescence spectra, it is obvious that the optimum ZnPc and CoPc concentrations are 5 μg/mL and the rGO is 1 μg/mL. This ratio is the maximum interaction amount of rGO and MPc compound. Characterization processes and sensing properties were performed for rGO/MPc hybrids prepared at these ratios. In addition, we have investigated the sonication effect on the formation of the rGO/ZnPc and rGO/CoPc hybrid systems using the fluorescence spectra. After the sonication time experiments, the formation was obtained in 25 min in both rGO/phthalocyanine hybrid structure.

Fig. 4 shows the scanning electron microscopy (SEM) of the rGO/CoPc (A, B) and rGO/ZnPc (C, D) in different magnitudes. SEM images show an interconnected porous structure. That is an irregular mesh pattern formation of CoPc and ZnPc were observed by anchoring on the surface of rGO like a human bone structure [42]. While ZnPc was densely and extensively distributed on the surface of rGO, a partial distribution was observed in CoPc.

We also measured the size of the pores observed in the images of the hybrids in SEM from approximately 100 points and give the results below with their standard deviations. rGO/CoPc hybrid structure has a wide range of distribution of produced pores that decreases the total surface area while also deteriorating the pore distribution. The analyzed pore distribution was found to be about 2.87 ± 1.67 μm which stands in a high deviation level. There were even 7.75 μm (max) pores as well as 0.85 μm (min) pore sizes. The connectivity was low and the specific area therefore should be lower. rGO/ZnPc hybrid was found to be much lower

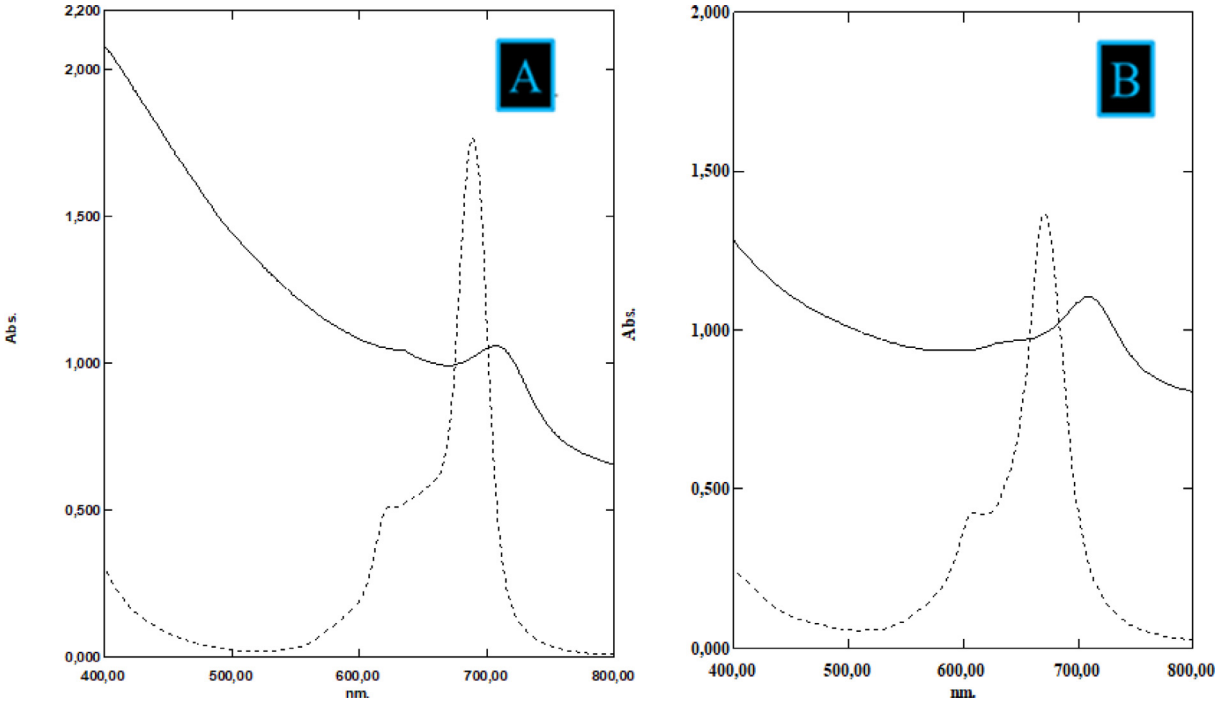

Fig. 2. Absorption spectra of (**A**) ZnPc (5 μg/mL) (—) and rGO/ZnPc hybrid (1 μg/mL / 5 μg/mL) (–) (**B**) CoPc (5 μg/mL) (—) and rGO/CoPc hybrid (1 μg/mL / 5 μg/mL) (–) in DMSO.

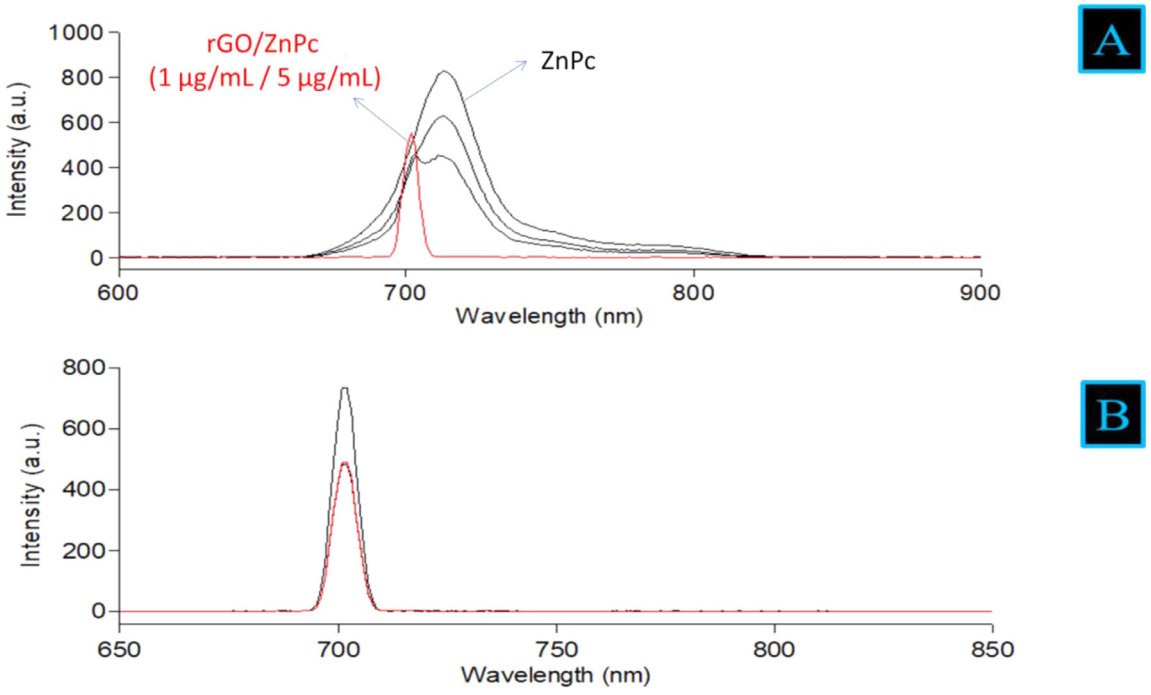

Fig. 3. (**A**) Fluorescence spectra of DMSO solution of ZnPc (5 μg/mL) against different concentrations of rGO. [rGO concentrations: 0.005 μg/mL; 0.05 μg/mL; 0.5 μg/mL; 1 μg/mL]. (**B**) Fluorescence spectra of rGO/CoPc hybrid in DMSO with different sonication times (CoPc-5 μg/mL; GO-0.05 μg/mL). [Sonication time (from up to down): 20, 25, 30 min]. (Exctitation wavelength: 700 nm).

than rGO/CoPc as 1.34 ± 0.86 μm pore size distribution. The maximum pore size was 5.53 μm while the minimum pore size was 0.49 μm. Table 1 shows the pore size distribution of both produced rGO/MPcs.

As illustrated in Fig. 5, the rGO/ZnPc has much lower mean pore size than rGO/CoPc which may be attributed to the better π-π stacking bonds as well as higher surface area. As the surface area and interaction between materials increase, the charge carrier capacity and mobility is predicted to be higher. Since the total area of pores are increased for smaller pores then it may be concluded that the density is increased in total volume and interaction between the connected finer grains, the charge carrying capacity is also increased due to higher amount of materials in unit volume. The coarser the pores, the lower the density, as a result, the charge

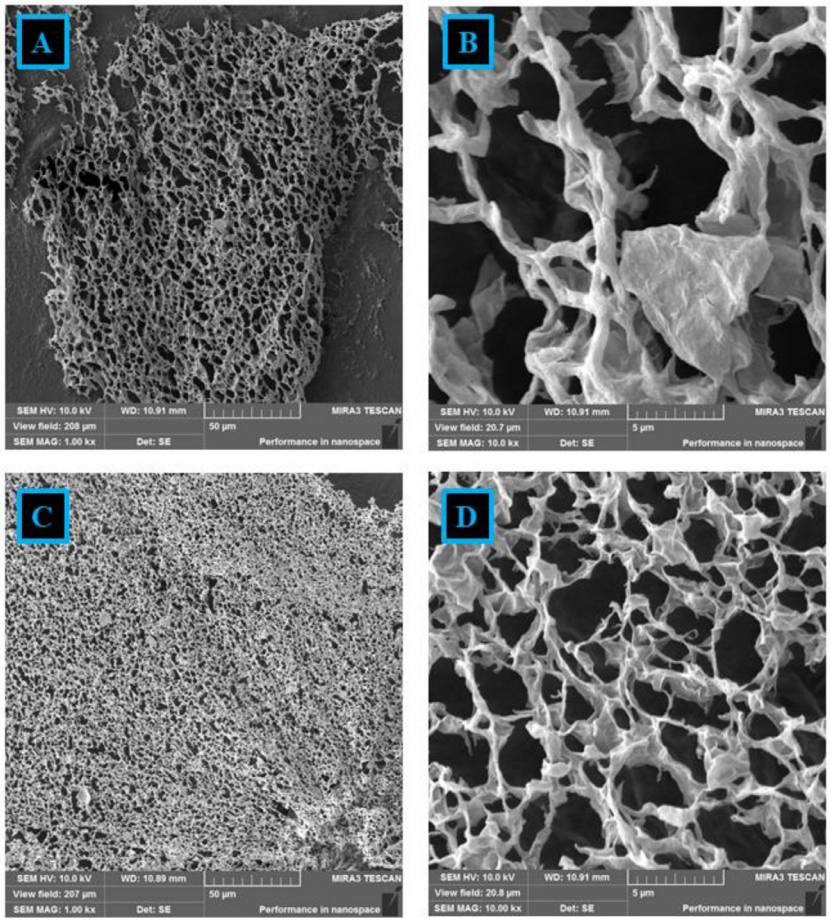

Fig. 4. The scanning electron microscopy images of (**A-B**) rGO/CoPc (1 µg/mL / 5 µg/mL) and (**C, D**) rGO/ZnPc (1 µg/mL / 5 µg/mL) with different magnitudes.

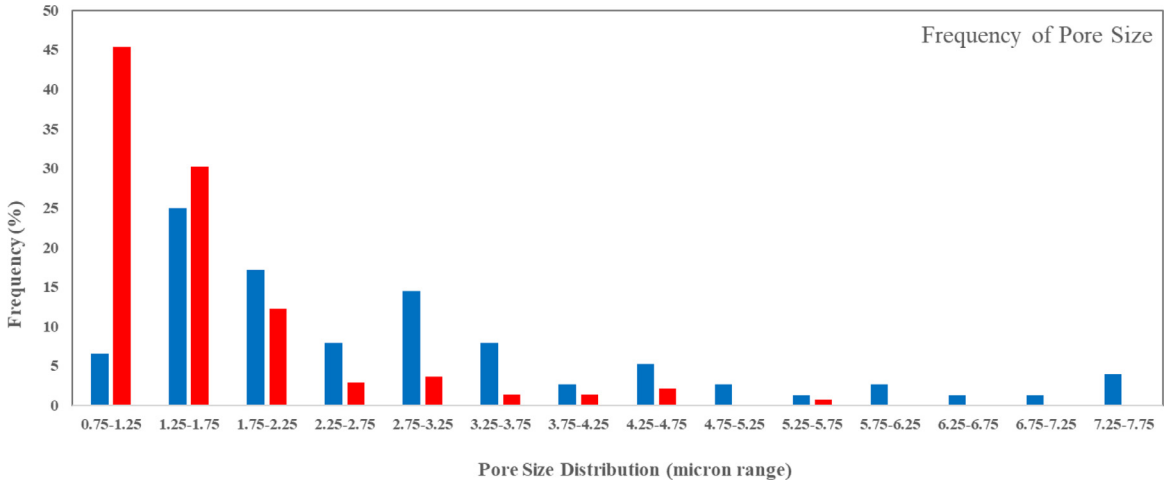

Fig. 5. Pore size distribution plot observed in SEM images of rGO/CoPc (blue line) and rGO/ZnPc hybrids (red line).

Table 1
Pore sizes and standard deviations from SEM images of hybrids.

Hybrid Structure	Minimum value (µm)	Maximum value (µm)	Mean value	Standard deviations
rGO/CoPc	0.85	7.75	2.87	1.67
rGO/ZnPc	0.49	5.53	1.34	0.86

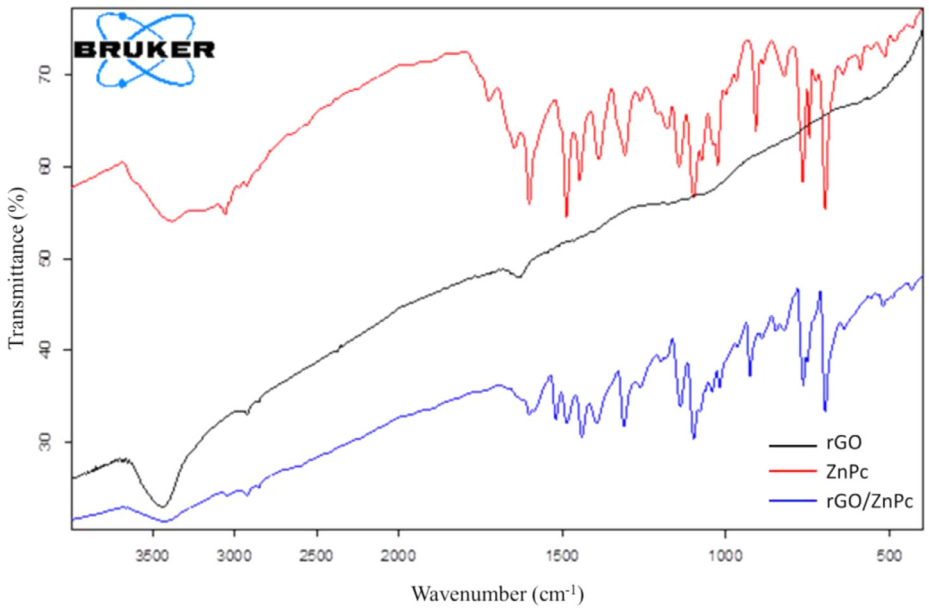

Fig. 6. FT-IR spectra of rGO, ZnPc, rGO/ZnPc (1 µg/mL / 5 µg/mL).

carrier density is also decreased. This may also be attributed to the contact area increase and possible increase in mean free path of electrons to conduct better.

Fig. 6 compares the FT-IR spectrum of the rGO, ZnPc and rGO/ZnPc hybrid. In the FT-IR spectrum of rGO, bands of -OH stretching, skeletal vibrations of unoxidized graphitic areas, -OH deformations of C-OH groups and stretching vibrations of CO groups were observed as broad [[43],[44]]. After its interaction with rGO and ZnPc or CoPc, it was observed that the intensity of the bands associated with their oxygen functionalities decreased. As a result of the formation of rGO/ZnPc and rGO/CoPc hybrid structures, it was observed that the bands showed general shift in the FT-IR spectra. It can be thought that this situation occurs as a result of gaining electron density due to electron transfer between rGO and phthalocyanine [45]. In addition, bands at approximately 1600-700 cm^{-1} in the FT-IR spectra of hybrid structures show the characteristic fingerprint region of ZnPc and CoPc. This shows the formation of hybrids of rGO and phthalocyanine [45].

3.2. Gas sensing measurements

Volatile organic compound sensing capabilities of rGO, rGO/ZnPc, and rGO/CoPc hybrid-based sensors deposited onto the Au interdigal electrodes were carefully investigated by using ammonia, acetone, ethanol, methanol, and butanol as the target molecules. The rationale behind the selection of these analytes as target molecules is that these analytes are indicators of some cancer types, especially early diagnosis of lung cancer and kidney failure. As a representative result, the response and recovery characteristics of these sensors to ammonia vapor with various concentration of ammonia between 30 and 210 ppm at room temperature (27 °C) is depicted in Fig. 7. As can be clearly seen from Fig. 7, upon exposure to ammonia molecules, the sensor current initially increases rapidly and over time the rate of increase in the sensor current decreases and tends to go to steady state value. After 5 min. exposure to ammonia vapor, purging with carrier gas leads to an initial fast decrease followed by a slow drift and the current reaches its initial value after the ammonia vapor is turned off for hybrid sensors. While the sensor current returns to its baseline values within 5 min when the ammonia gas vapor is turned off in hybrid-based sensors, the recovery does not occur in the rGO-based sensor during this time interval. The same type of response–recovery characteristics were also obtained for other volatile organic compound vapors investigated. The rapid increase in sensor current at initial stage of exposure and then the slowing rate of increase can be explained as follows; it is believed that the magnitude of the sensor response is proportional to the number of adsorption sites occupied by target molecules on the sensing layer. The exposure of the sensor surface to carrier gas leads to desorption of the adsorbed vapor molecules from the surface, decreasing the acceptor concentration and thus the sensor current.

This means that the sensor current is dominated by the number of active adsorption sites onto the sensing layer and the rate of charge transfer between target molecules and these sites. In the first stage of exposure, due to the presence of large number of unoccupied adsorption sites onto the sensing layer, the number of adsorbed gas molecules will be very large and accordingly the charge transfer rate will be high. On the other hand, the number of the unoccupied adsorption sites on the surface of the sensing layer is expected to decrease with the exposure time. Thus, a reduction in adsorption and charge transfer processes occurs and rate of increase in sensor current slowdown.

To fully clarify the mechanism of the adsorption and desorption between ammonia and rGO/Pc hybrids, it is important to understand the interactions between the rGO/Pc surface and the adsorbate molecules. Adsorption energies and the charge transfer number of the composite systems were studied experimentally and first-principle calculations by Peng et al. [46]. The gas sensor based on pristine graphene with conductance type was studied and time response of conductance measurements showed a quickly and largely increased conductivity when the sensor was exposed to ammonia gas produced by a bubble system. It was also reported that the conductance of the graphene based sensor increased ~22.5 % when exposed to 5 ppm ammonia. It was concluded that there is a slight charge transfer from the molecule to the graphene surface in the U orientation and an extremely slight charge transfer from graphene to NH_3 molecule in the D orientation.

The sensor response is an important characteristic for the application of sensors at room temperature. The variations in the sensor response with ammonia concentrations between 30 and 210 ppm of ammonia vapor was examined and the results are presented in

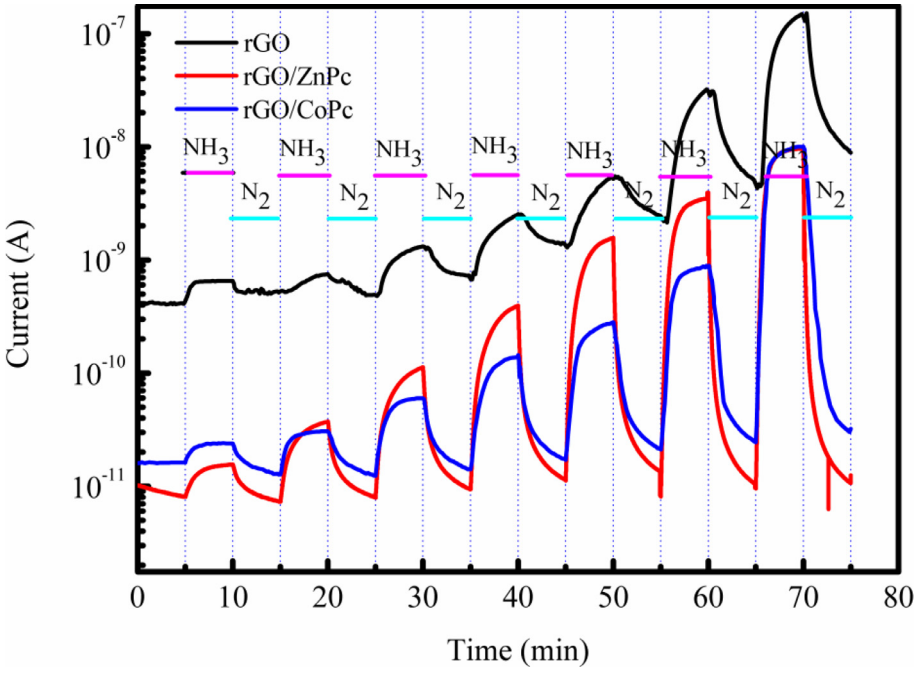

Fig. 7. Room temperature response-recovery characteristics of the sensors towards ammonia vapor.

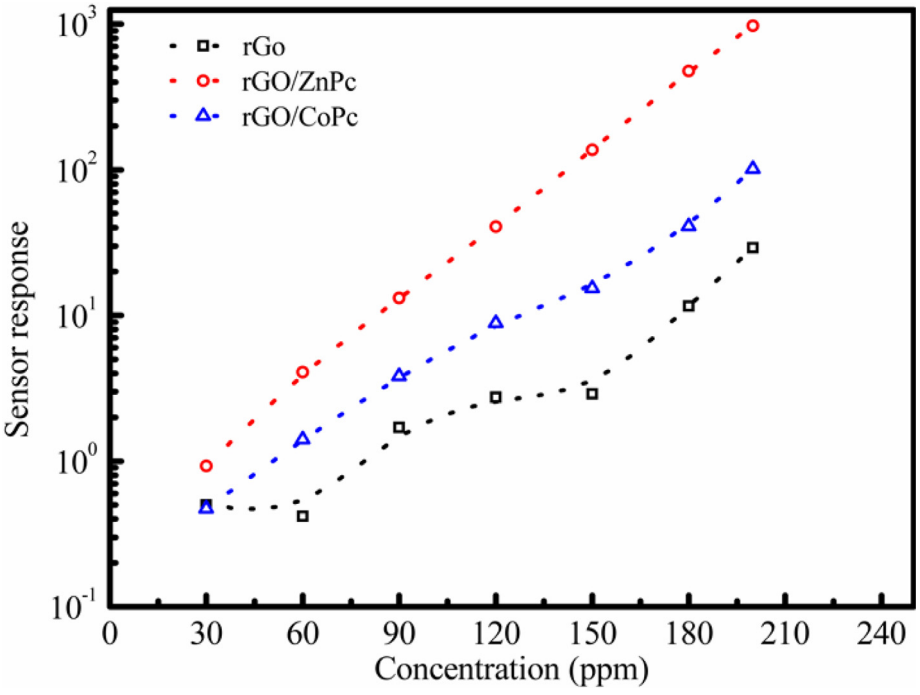

Fig. 8. The variations in the sensor response with ammonia concentrations.

Fig. 8. Here, the sensor response (R) was defined as,

$$R = \frac{\Delta I}{I_0}$$

Where ΔI is the change in the sensor current at a certain concentration of the target gas molecules, and I_0 is the current of the device in the carrier gas environment.

The response of the sensors increases with respect to ammonia concentrations ranging from 30 to 210 ppm (Fig. 8). The highest response has been recorded using rGO/ZnPc coated sensor, while the rGO based sensor showed the lowest response to ammonia vapor. The results indicated that enhance the response to ammonia due to strong interactions between the rGO/MPc hybrid surface and ammonia. The SEM photographs in Fig. 4 show that rGO/ZnPc has a lower average pore size and higher surface area than rGO/CoPc. It can be said that the interaction will increase as the surface area increases. Accordingly, the difference in the response of the rGO/MPc introduced based sensors reveals that the surface morphologies play a dominant role in the adsorption processes. To further investigate the ammonia sensing performance of rGO, rGO/ZnPc, and rGO/CoPc hybrid sensors, we have recorded the response-recovery curve of the sensors for a repeated ammonia concentration of 180 ppm for many times. When the sensors are

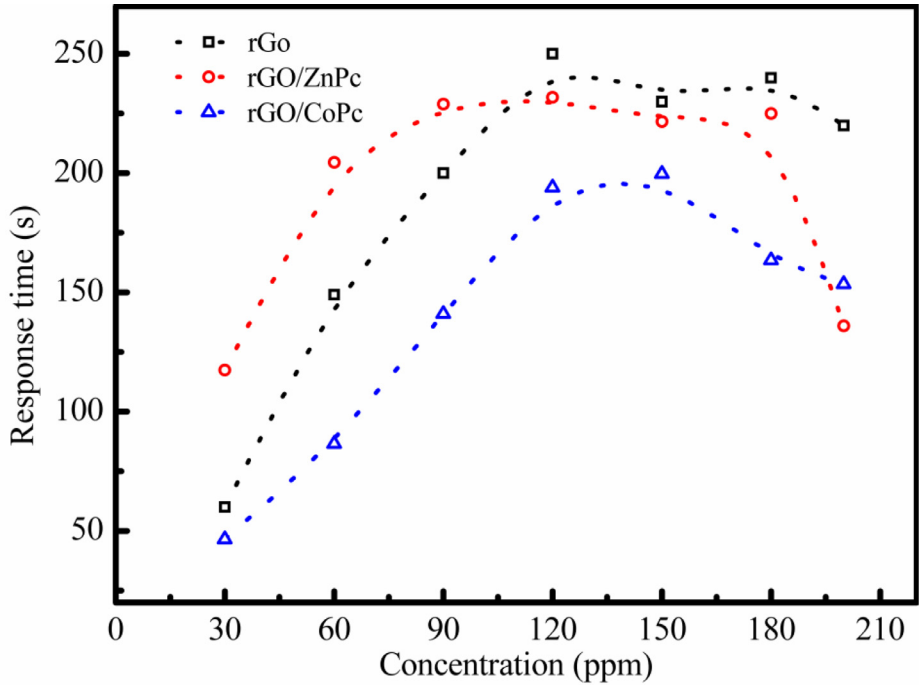

Fig. 9. The variation of response time with ammonia concentration for rGO/ZnPc hybrid sensor.

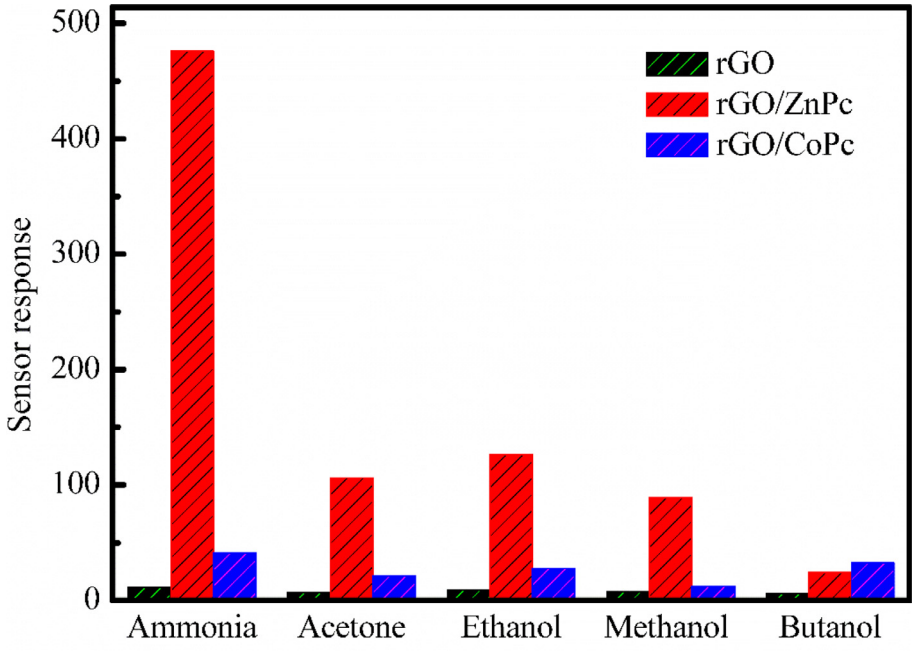

Fig. 10. The effect of Pc incorporation on sensing performance of rGO based sensors.

exposed to the same concentration of ammonia vapor 7 times, the same current values are observed with a 2% deviation each time in the rGO/ZnPc and rGO/CoPc hybrid-based sensors, while this deviation is 18% in the rGO-based sensor. The same value of the sensor current on every time exposure for rGO/ZnPc and rGO/CoPc hybrid-based sensors show that the response-recovery curves are highly reproducible.

One of the most important performance parameter for a gas sensor is the limit of detection (LOD), which is defined as the lowest concentration of an analyte in a sensing element that can be consistently detected with a stated probability [47]. The limit of detection (LOD) for rGO/ZnPc hybrid was estimated to be 82 ppb at 25°, according to following equation.

$$LOD = \frac{N_{rms}}{S}$$

where N_{rms} is the standart deviation of the noise and S is the slope of linear fitting of response-recovery characteristics. In order to certify the effects of the central metal ion on the LOD, the LOD for ammonia vapour of rGO and rGO/CoPc hybrids were also obtained and it was obtained to be 233 ppb and 140 ppb, respectively.

Another important performance indicator in sensor applications is the response time of the sensor. The response time of a sensor is defined as the time it takes for the change in sensor current

to reach 90% of its maximum value. It should be mentioned here that the smaller value of response time of a sensor indicates its rapid response characteristic. As a representative result, the variation of the response time with ammonia vapor for all sensors investigated is shown in Fig. 9. As can be clearly seen from Fig. 9, for all the sensors examined, the response time is an increasing function of the ammonia concentration for low values of ammonia concentration, while it decreases after a certain value of the ammonia concentration, depending on the sensing layer used as sensing element. The response time for 120 ppm ammonia vapor were approximately 250 s, 230 s and 190 s for rGO, rGO/ZnPc, and rGO/CoPc based sensors, respectively. It is well known that the response time in Pc based sensors depend on several factors that include the chemical nature of Pc, the polymorphic phase of the microcrystallites comprising the film, the film thickness, molecular structure of the analyte molecules, etc. These results may suggest that the response time for MPc incorporated rGO based sensor is controlled by the central metal ion incorporated into the Pc ring.

The selectivity is another important characteristic for the application of sensors at room temperature. Therefore, acetone, ethanol, methanol, and butanol sensing performance of the sensors were also investigated and sensor responses for these vapors are shown in Fig. 10. Among the volatile organic compound vapors whose detection properties were investigated, the rGO/ZnPc based sensor exhibited the highest response to all volatile organic compound vapors investigated. Fig. 10 clearly shows that rGO/ZnPc hybrid-based sensor has a great potential for the selective detection of ammonia vapor.

4. Conclusions

In this study, novel 4-pyridinyl-oxadiazole tetrasubstituted zinc and cobalt phthalocyanine compounds were synthesized as a result of the tetramerization reaction of the phthalonitrile derivative and further characterized. rGO/ZnPc and rGO/CoPc hybrids were characterized by UV-Vis, fluorescence spectroscopy and SEM images. The measurement results confirm that the prepared non-covalent rGO/ZnPc and rGO/CoPc hybrid structures are formed by strong π–π interaction. Based on the preliminary studies discussed above, the rGO/ZnPc hybrid sensors displayed superior response. Therefore, the rGO/ZnPc hybrid is promising candidates for use as an ammonia sensing layer. Our studies have demonstrated that rGO/ZnPc has 43-fold sensor response to ammonia, also we have found out that rGO/ZnPc has moderate effect on acetone, ethanol and methanol. It can be said that the rGO/ZnPc hybrid compound has the potential to be used as a breath sensor in the medical diagnosis of diseases, especially in the early diagnosis of lung cancer and kidney failure.

Declaration of Competing Interest

The authors declare that they have no known competing financial interests or personal relationships that could have appeared to influence the work reported in this paper.

CRediT authorship contribution statement

Ebru Yabaş: Conceptualization, Methodology, Validation, Formal analysis, Investigation, Resources, Data curation, Software, Supervision, Project administration, Visualization. **Emre Biçer:** Software, Investigation, Visualization. **Ahmet Altındal:** Software, Validation, Formal analysis, Investigation, Resources, Data curation, Writing – review & editing, Supervision.

Data Availability

No data was used for the research described in the article.

Acknowledgments

In this study, the laboratory facilities of the Advanced Technology Application and Research Center of Sivas Cumhuriyet University (CÜTAM) were used. This work was partially supported by Sivas Cumhuriyet University Scientific Research Projects Commission with the projects Nos. İMYO-005 and F-398.

References

[1] G. Torre, G. Bottari, U. Hahn, T. Torres, Functional phthalocyanines: synthesis, nanostructuration, and electro-optical applications, Struct. Bond. 135 (2010) 1–44.
[2] T.H. Kim, H.J. Kim, C.G. Kwak, W.H. Park, T.S. Lee, Aromatic oxadiazole-based conjugated polymers with excited-state intramolecular proton transfer: their synthesis and sensing ability for explosive nitroaromatic compounds, J. Polym. Sci. A 44 (2006) 2059–2068.
[3] X. Tang, M. Debliquy, D. Lahem, Y. Yan, J.P. Raskin, A Review on functionalized graphene sensors for detection of ammonia, Sensors 21 (2021) 1443–1469.
[4] N.I. Zaaba, K.L. Foo, U. Hashim, S.J. Tan, W.W. Liu, C.H. Voon, Synthesis of graphene oxide using modified hummers method: solvent influence, Proced. Eng. 184 (2017) 469–477.
[5] X. Zhou, X. Wang, B. Wang, Z. Chen, C. He, Y. Wu, Preparation, characterization and NH_3-sensing properties of reduced graphene oxide/copper phthalocyanine hybrid material, Sens. Actuators B 193 (2014) 340–348.
[6] Z. Chen, J. Wang, Y. Wang, Strategies for the performance enhancement of graphene-based gas sensors: a review, Talanta 235 (2021) 122745–122756.
[7] T. Patois, J.B. Sanchez, F. Berger, P. Fievet, O. Segut, V. Moutarlier, M. Bouvet, B. Lakard, Elaboration of ammonia gas sensors based on electrodeposited polypyrrole-cobalt phthalocyanine hybrid films, Talanta 117 (2013) 45–54.
[8] Z. Jiang Guo, B. Wang, X. Wang, Y. Li, S. Gai, Y. Wua, XLi Cheng, A high-sensitive room temperature gas sensor based on cobalt phthalocyanines and reduced graphene oxide nanohybrids for the ppb-levels of ammonia detection, RSC Adv. 9 (2019) 37518–37525.
[9] A. Kumar, R. Meunier-Prest, M. Bouvet, Organic heterojunction devices based on phthalocyanines: a new approach to gas chemosensing, Sensors 20 (2020) 4700–4724.
[10] B. Wang, X. Wang, X. Li, Z. Guo, X. Zhou, Y. Wu, The effects of amino substituents on the enhanced ammonia sensing performance of PcCo/rGO hybrids, RSC Adv. 8 (2018) 41280–41287.
[11] X. Li, B. Wang, X. Wang, X. Zhou, Z. Chen, C. He, Z. Yu, Y. Wu, Enhanced NH_3-sensitivity of reduced graphene oxide modified by tetra-α-isopentyloxymetallophthalocyanine derivatives, Nanoscale Res. Lett. 10 (1) (2015) 373–383.
[12] Z. Yu, B. Wang, Y. Li, D. Kang, Z. Chen, Y. Wu, The effect of rigid phenoxyl substituent on the NH_3-sensing properties of tetra-α-(4-tert-butylphenoxyl)-metallophthalocyanine/reduced graphene oxide hybrids, RSC Adv. 7 (36) (2017) 22599–22609.
[13] S. Kumar, N. Kaur, A.K Sharma, A. Mahajan, R.K. Bedi, Graphene oxide when decorated with copper phthalocyanine nanoflowers, RSC Adv. 7 (41) (2017) 25229–25236.
[14] B. Wang, X. Wang, Z. Guo, S. Gai, Y. Li, Y. Wu, A highly sensitive ppb-level H_2S gas sensor based on fluorophenoxy-substituted phthalocyanine cobalt/rGO hybrids at room temperature, RSC Adv. 11 (2021) 5993–6001.
[15] G.H. Lu, L.E. Ocola, J.H. Chen, Reduced graphene oxide for room-temperature gas sensors, Nanotechnology 20 (2009) 445502–445511.
[16] W. Li, X. Geng, Y. Guo, J. Rong, Y. Gong, L. Wu, X. Zhang, P. Li, J. Xu, G. Cheng, M. Sun, L. Liu, Reduced graphene oxide electrically contacted graphene sensor for highly sensitive nitric oxide detection, ACS Nano 5 (2011) 6955–6961.
[17] A. Midya, S. Mukherjee, S. Roy, S. Santra, N. Manna, S.K. Ray, Selective chloroform sensor using thiol functionalized reduced graphene oxide at room temperature, Mater. Res. Express 5 (2018) 025604–025619.
[18] S. Yoo, X. Li, Y. Wu, W. Liu, X. Wang, W. Yi, Ammonia gas detection by tannic acid functionalized and reduced graphene oxide at room temperature, J. Nanomater. 2014 (2014) 1–6.
[19] E. Kakı, A.R. Özkaya, A. Altındal, B. Salih, Ö. Bekaroğlu, Synthesis, characterization, electrochemistry and VOC sensing properties of novel metallophthalocyanines with four cyclohexyl-phenoxyphthalonitrile groups, Sens. Actuators B 188 (2013) 1033–1042.
[20] F.I. Bohrer, A. Sharoni, C. Colesniuc, J. Park, I.K. Schuller, A.C. Kummel, W.C. Trogler, Gas sensing mechanism in chemiresistive cobalt and metal-free phthalocyanine thin films, J. Am. Chem. Soc. 129 (2007) 5640–5646.
[21] A. Maity, A.K. Raychaudhuri, B. Ghosh, High sensitivity NH_3 gas sensor with electrical readout made on paper with perovskite halide as sensor material, Sci. Rep. 9 (2019) 7777–7786.
[22] G. Gregis, J.B. Sanchez, I. Bezverkhyy, G. Weber, F. Berger, V. Fierro, J.P. Bellat, A. Celzar, Detection and quantification of lung cancer biomarkers by a micro–analytical device using a single metal oxide-based gas sensor, Sens. Actuators B 255 (2018) 391–400.
[23] P. Fuchs, C. Loeseken, J.K. Schubert, W. Miekisch, Breath gas aldehydes as biomarkers of lung cancer, Int. J. Cancer 126 (2010) 2663–2670.

[24] H. Haick, Y.Y. Broza, P. Mochalski, V. Ruzsanyi, A. Amann, Assessment, origin, and implementation of breath volatile cancer markers, Chem. Soc. Rev. 43 (2014) 1423–1449.
[25] K.H. Kim, S.A. Jahan, E. Kabir, A review of breath analysis for diagnosis of human health, Trend. Anal. Chem. 33 (2012) 1–8.
[26] C.D. Natale, R. Paolesse, E. Martinelli, R. Capuano, Solid-state gas sensors for breath analysis: a review, Anal. Chim. Acta 824 (2014) 1–17.
[27] Y. Adıgüzel, H. Kulah, Breath sensors for lung cancer diagnosis, Biosens. Bioelectron. 65 (2015) 121–138.
[28] A.G. Dent, T.G. Sutedja, P.V. Zimmerman, Exhaled breath analysis for lung cancer, J. Thorac. Dis. 5 (2013) 540–550.
[29] G. Zhao, M. Li, Ni-doped MoS_2 biosensor: a promising candidate for early diagnosis of lung cancer by exhaled breathe analysis, Appl. Phys. A 124 (2018) 751–759.
[30] W.L.F. Armarego, C.L.L. Chai, Purificaiton of Laboratory Chemicals, 3rd ed., Butterworth/Heinemann, Tokyo, 2003 5.
[31] E. Bağda, E. Yabaş, E. Bağda, Analytical approaches for clarification of DNA-double decker phthalocyanine binding mechanism: as an alternative anticancer chemotherapeutic, Spectrochim. Acta A 172 (2017) 199–204.
[32] S. Şahin, S. Altun, A. Altındal, Z. Odabaş, Synthesis of novel azo-bridged phthalocyanines and their toluene vapour sensing properties, Sens. Actuators B 206 (2015) 601–608.
[33] D.E. Bornside, C.W. Macosko, L.E. Scriven, Spin coating of a PMMA/chlorobenzene solution, J. Electrochem. Soc. 138 (1991) 317.
[34] J. Riddick, A. Bunger, A. Weissberger (Ed.), Organic Solvents in Techniques of Chemistry, 2, Wiley/Interscience, New York, 1970.
[35] E. Yabaş, M. Sülü, S. Saydam, F. Dumludağ, B. Salih, Ö. Bekaroğlu, Synthesis, characterization and investigation of electrical and electrochemical properties of imidazole substituted phthalocyanines, Inorg. Chim. Acta 365 (2011) 340–348.
[36] A. Yazıcı, C. Özkan, M.B. Gezer, A. Altındal, B. Salih, Ö. Bekaroğlu, Analysis of rectifying behavior of novel ball-type binuclearphthalocyanine based devices, Inorg. Chim. Acta 404 (2013) 40–48.
[37] T. Ceyhan, A. Altındal, A.R. Özkaya, B. Salih, Ö. Bekaroğlu, Novel ball-type four dithioerythritol bridged metallophthalocyanines and their water-soluble derivatives: Synthesis and characterization, and electrochemical, electrocatalytic, electrical and gas sensing properties, Dalton Trans. 39 (2010) 9801–9814.
[38] G.A. Gauna, J. Marino, M.C.G. Vior, L.P. Roguin, Awruch, Synthesis and comparative photodynamic properties of two isosteric alkyl substituted zinc(II) phthalocyanines, Eur. J. Med. Chem. 46 (2011) 5532–5539.
[39] M.S. Yar, M.W. Akhter, Synthesis and anticonvulsant activity of substituted oxadiazole and thiadiazole derivatives, Acta Pol. Pharm. 66 (2009) 393–397.
[40] T. Nyokong, E. Antunes, Influence of nanoparticle materials on the photophysical behavior of phthalocyanines, Coord. Chem. Rev. 257 (2013) 2401–2418.
[41] X.F. Zhang, X. Shao, π-π-Binding ability of different carbon nano-materials with aromaticphthalocyanine molecules: comparison between graphene, graphene oxide and carbon nanotubes, J. Photochem. Photobiol. A 278 (2014) 69–74.
[42] J. Will, L.C. Gerhardt, A.R. Boccaccini, Bioactive glass-based scaffolds for bone tissue engineering, Adv. Biochem. Eng. Biotechnol. 126 (2012) 195–226.
[43] P. Das, K. Chakraborty, S. Chakrabarty, S. Ghosh, T. Pal, Reduced graphene oxide - zinc phthalocyanine composites as fascinating material for optoelectronic and photocatalytic applications, ChemistrySelect 2 (2017) 3297–3305.
[44] N. Wu, X. She, D. Yang, X. Wu, F. Su, Y. Chen, Synthesis of network reduced graphene oxide in polystyrene matrix by a two-step reduction method for superior conductivity of the composite, J. Mater. Chem. 22 (2012) 17254–17261.
[45] I.S. Hosu, Q. Wang, A. Vasilescu, S.F. Peteu, V. Raditoiu, S. Railian, V. Zaitsev, K. Turcheniuk, Q. Wang, M. Li, R. Boukherroub, S. Szunerits, Cobalt phthalocyanine tetracarboxylic acid modified reduced graphene oxide: a sensitive matrix for the electrocatalytic detection of peroxynitrite and hydrogen peroxide, RSC Adv. 5 (2015) 1474–1484.
[46] Z. Zhang, X. Zhang, W. Luo, H. Yang, Y. He, Y. Liu, X. Zhang, G. Peng, Study on adsorption and desorption of ammonia on graphene, Nanoscale Res. Lett. 10 (2015) 359.
[47] D.A. Armbruster, T. Pry, Limit of blank, limit of detection and limit of quantitation, Clin. Biochem. Rev. 29 (2008) S49–S52.